Alexandria Engineering Journal (2023) 65, 897–908

HOSTED BY

Alexandria University

Alexandria Engineering Journal

www.elsevier.com/locate/aej
www.sciencedirect.com

ORIGINAL ARTICLE

Entropy analysis of magnetized ferrofluid over a vertical flat surface with variable heating

Hanifa Hanif [a,b,*], Sharidan Shafie [b,*], Noraihan Afiqah Rawi [b], Abdul Rahman Mohd Kasim [c]

[a] Department of Mathematics, Sardar Bahadur Khan Women's University, Quetta, Pakistan
[b] Department of Mathematical Sciences, Faculty of Science, Universiti Teknologi Malaysia, 81310 Johor Bahru, Johor, Malaysia
[c] Centre for Mathematical Sciences, Universiti Malaysia Pahang, Lebuhraya Tun Razak, 26300 Gambang Kuantan, Pahang Darul Makmur, Malaysia

Received 14 June 2022; revised 12 September 2022; accepted 27 September 2022
Available online 22 October 2022

KEYWORDS

Nanofluid;
Entropy generation;
Magnetohydrodynamic;
Finite difference method

Abstract This research analyzes the entropy generation in a two-dimensional flow of magnetized ferrofluid with variable wall temperature in the presence of heat generation. The mathematical model is designed to consolidate cylindrical-shaped Fe_3O_4-nanoparticles in pure water. An implicit finite difference is used to obtain the desired numerical solutions. The effects of nanoparticle volume concentration, magnetic parameter, heat generation, and power index on fluid velocity, temperature, entropy generation, and Bejan number are illustrated graphically. The entropy generation increased when the Brinkmann number increased; however, it decreased when the temperature difference decreased. For the authenticity of the current research, the obtained findings are compared with the previously existing results under certain conditions, and a good coexistence is achieved.

1. Introduction

Numerous industrial and technical fields are using nanotechnology because it plays a leading role in advanced technologies. Nanotechnology depends on the capacity to create, manipulate, and fabricate materials at the nanoscale, and nanomaterials are the name given to these materials. The contribution of nanomaterials in enhancing the heat transfer mechanism is appreciable. On the other hand, the thermal conductivity of traditional heat transfer fluid is inadequate to acquire the desired heat transfer rates. Therefore, researchers are using nanoparticles to increase the thermal efficiency of heat transfer fluids. The mixture of nanoparticles and fluid is called nanofluid, introduced by Choi and Eastman [1]. Several studies have been performed on convective heat transfer fluid flow using nanomaterials over the past few decades [2–7]. Nanofluids with superparamagnetic nanoparticles are named ferrofluids. These are frequently known as functional and valuable fluids in which a magnetic field is applied to fluid flow, thereby improving the carrier fluid's thermal performance. Because of their potential use in the process of heat transmission, they have attracted a lot of study attention. Pattnaik

* Corresponding authors.
E-mail addresses: hanifahanif@outlook.com (H. Hanif), sharidan@utm.my (S. Shafie).
Peer review under responsibility of Faculty of Engineering, Alexandria University.

https://doi.org/10.1016/j.aej.2022.09.052

et al. [8] noticed an increment in the temperature of Fe_3O_4/water ferrofluid due to the radiative heat energy emitted by the particle. In a study, Hanif et al. [9] observed that heat transfer rates of Fe_3O_4/water are higher than Cu/water in the presence of heat absorption. The flow of Fe_3O_4/water ferrofluid between two spinning surfaces has been studied by Shahzad et al. [10]. During the study, they found that heat transfer rates increase dramatically for the Fe_3O_4/water compared to the conventional fluid as the concentration of nanoparticles increases. We also refer to some investigations considering ferrofluid [11–13].

Heat transfer phenomena in the presence of a magnetic field have numerous applications in several industries, including manufacturing and engineering, such as crystal growth, paper production, polymer extrusion, artificial fibers, plastic films, etc. Due to these significant applications, magnetohydrodynamics (MHD) in heat transfer owned special attention from researchers and engineers. Several research studies have been conducted to explore the influence of a magnetic field on the heat transfer characteristics of conventional fluids. Hanif and Shafie investigated MHD Maxwell fluid in the presence of Joule heating and viscous dissipation [14,15]. Their results showed that the magnetic field causes a downturn in the velocity but increases the temperature. Pattnaik et al. [16] analyzed the MHD flow of Au/water in a permeable channel. Saqib et al. [17] utilized the Cattaneo-Friedrich concept to analyze the influence of inclined MHD Flow of Maxwell fluid. Some fruitful articles on MHD flow are present in [18–20].

In recent years, it has proven possible to create the best engineering system designs by limiting entropy formation using the second law of thermodynamics. Entropy generation is a unit of measurement for the amount of irreversibility that builds up throughout a process. Entropy generation may therefore be a metric for assessing the performance of engineering devices [21]. Numerous forms of irreversibility contribute to entropy generation, including temperature gradient, fluid frictions, and convective heat transfer qualities. Entropy analysis is famous in various sectors, including spinning reactors, heat transfer equipment, nuclear fuel rod cooling, and solar energy collectors. For instance, Khosravi et al. [22] used neural networks to analyze the entropy production of hybrid nanofluid flow in a wavy microchannel solar receiver. Marzougui et al. [23] calculated the irreversibility of convective nanofluid flow in the presence of a magnetic field in a cavity with chamfers. A depletion in viscous and thermal entropy generation occurred for an increased Hartmann number with a fixed angle of inclination of the magnetic field. Jamshed [24] noticed an exaggerated entropy in MHD Maxwell nanofluid on adding nanoparticles. Tayebi et al. [25] investigated the irreversibility of MHD nanofluid flow between two differentially heated circular cylinders. Their results showed that irreversibility due to thermo-effects is prominent for low Rayleigh numbers. Moreover, the irreversibility due to thermo-effects is no longer the main contributor to total entropy generation when Rayleigh values increase. Nakhchi and Rahmati [26] explored the effects of transverse-cut twisted tapes on the thermal properties and entropy generation of Cu/water nanofluid within a uniform-wall heat exchanger. Jamshed et al. [27] analyzed entropy generation in a second-grade fluid and noticed an incredible increment in entropy due to Reynolds and Brinkman numbers. Contemporary works on convective heat transfer and entropy generation problems in different configurations can be found in [28–30].

The main objective of this investigation is to examine the irreversibility problem in nanofluid flow in the presence of a magnetic field. Numerous scholars have highlighted the irreversibility of MHD fluid flow. But unsteady flow problems have been frequently disregarded. Further, solving time-dependent partial differential equations (PDEs) using similarity transformations is common, but solving PDEs is rare. Therefore, the present research analyzes the irreversibility process in an unsteady nanofluid flow using the finite difference method. It is worth mentioning the thermal and mechanical properties of a nanofluid depend on the selection of base fluid, volume concentration, type, size, and shape of nanoparticles. Even though the most common particles are spherical nanoparticles, they are insubstantial in terms of significance and applications. As a consequence, the cylindrical nanoparticles have been integrated with the current study. The novelty of the research increased by considering the effects of a magnetic field and heat generation.

2. Problem description

A convective heat transfer in magnetized Fe_3O_4/water ferrofluid with uniform velocity u_0 is considered. The surface of the geometry is taken as x-axis, and y-axis is assumed in the normal direction to the flow. A uniform-magnetic field $B = (0, B_0, 0)$ is applied normal to the flow direction, see Fig. 1. The flow is initiated with wall temperature $T_w(x)$in the presence of heat generation Q_0. If $(u(x, y, t), v(x, y, t))$ be the velocity components in (x, y) directions and $T(x, y, t)$ is the temperature then the governing equations using boundary layer and Boussinesq approximations are given as

$$u_x + v_y = 0, \tag{1}$$

$$\rho_{nf}\left(u_t + uu_x + vu_y\right) = \mu_{nf}u_{yy} - \sigma_{nf}B_0^2 u + g(\rho\beta)_{nf}(T - T_\infty), \tag{2}$$

$$(\rho C_p)_{nf}\left(T_t + uT_x + vT_y\right) = k_{nf}T_{yy} + Q_0(T - T_\infty). \tag{3}$$

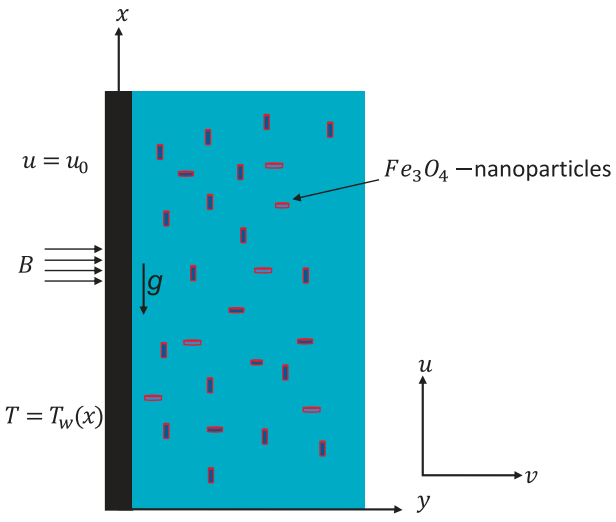

Fig. 1 Graphical representation.

The mathematical expression for nanofluid properties including density ρ_{nf}, dynamic viscosity μ_{nf}, thermal expansion β_{nf}, heat capacity at constant pressure $(C_p)_{nf}$, thermal conductivity k_{nf} and electrical conductivity σ_{nf} are given Table 1 and the thermo-physical properties of base fluid and nanoparticles are depicted in Table 2.

The initial and boundary conditions are given as below:

$$\begin{aligned} t \le 0: &\quad u(x,y,t) = v(x,y,t) = 0,\ T(x,y,t) = T_\infty, \\ t > 0: &\quad u(x>0,0,t) = u_0,\ v(x,0,t) = 0,\ T(x,0,t) = T_\infty + cx^n, \\ &\quad u(0,y,t) = u(x,\infty,t) = 0,\ T(0,y,t) = T(x,\infty,t) = T_\infty. \end{aligned} \tag{4}$$

Using the following non-dimensional quantities:

$$x^* = \tfrac{xu_0}{\nu_f},\quad y^* = \tfrac{yu_0}{\nu_f},\quad t^* = \tfrac{tu_0^2}{\nu_f},\quad u^* = \tfrac{u}{u_0},\quad v^* = \tfrac{v}{u_0},\quad T^* = \tfrac{T-T_\infty}{T_w-T_\infty}. \tag{5}$$

into Eqs. 1, 2 and 3, gives us (for the sake of simplicity $*$ is removed)

$$u_x + v_y = 0, \tag{6}$$

$$\phi_1\left[u_t + uu_x + vu_y\right] = \phi_2 u_{yy} - \phi_3 Mu + \phi_4 RiRe^{-1}T, \tag{7}$$

$$\phi_5\left[T_t + uT_x + vT_y\right] = \phi_6 Pr^{-1}T_{yy} + QT, \tag{8}$$

where

$$\begin{aligned} \phi_1 &= (1-\varphi) + \varphi\tfrac{\rho_s}{\rho_f}, & \phi_2 &= 1 + 13.5\varphi + 904.4\varphi^2, & \phi_3 &= \tfrac{\sigma_{nf}}{\sigma_f}, \\ \phi_4 &= (1-\varphi) + \varphi\tfrac{(\rho\beta)_s}{(\rho\beta)_f}, & \phi_5 &= (1-\varphi) + \varphi\tfrac{(\rho C_p)_s}{(\rho C_p)_f}, & \phi_6 &= \tfrac{k_{nf}}{k_f}, \\ M &= \tfrac{B_0^2\sigma_f\nu_f}{\rho_f u_0^2}, & Ri &= \tfrac{g\beta_f(T_w-T_\infty)L}{u_0^2}, & Re &= \tfrac{u_0 L}{\nu_f}, \\ Pr &= \tfrac{\nu_f}{\alpha_f}, & \alpha_f &= \tfrac{k_f}{(\rho C_p)_f}, & Q &= \tfrac{Q_0\nu_f}{(\rho C_p)_f u_0^2}. \end{aligned} \tag{9}$$

Here $\phi_1 - \phi_6$, M, Ri, Re, Pr, α and Q denote the nanofluid constants, magnetic parameter, Richardson number, Reynolds number, Prandtl number, thermal diffusivity, and heat generation/absorption parameter, respectively. The initial and boundary conditions are given below:

$$\begin{aligned} t \le 0: &\quad u(x,y,t) = v(x,y,t) = 0,\ T(x,y,t) = 0, \\ t > 0: &\quad u(x>0,0,t) = 1,\ v(x,0,t) = 0,\ T(x,0,t) = x^n, \\ &\quad u(0,y,t) = u(x,\infty,t) = 0,\ T(0,y,t) = T(x,\infty,t) = 0. \end{aligned} \tag{10}$$

Table 1 Mathematical expression of nanofluid properties.

Properties	Nanofluid
Density	$\rho_{nf} = (1-\varphi)\rho_f + \varphi\rho_s$
viscosity	$\mu_{nf} = \mu_f(1 + 13.5\varphi + 904.4\varphi^2)$
Thermal expansion	$(\rho\beta)_{nf} = (1-\varphi)(\rho\beta)_f + \varphi(\rho\beta)_s$
Heat capacitance	$(\rho C_p)_{nf} = (1-\varphi)(\rho C_p)_f + \varphi(\rho C_p)_s$
Thermal conductivity	$\frac{k_{nf}}{k_f} = \frac{(k_s+(m-1)k_f)+(m-1)\varphi(k_s-k_f)}{(k_s+(m-1)k_f)-\varphi(k_s-k_f)}$ with $m = 3/\psi$, where $\psi = 0.62$
Electrical conductivity	$\frac{\sigma_{nf}}{\sigma_f} = 1 + \frac{3\varphi\left(\frac{\sigma_s}{\sigma_f}-1\right)}{\left(\frac{\sigma_s}{\sigma_f}+2\right)-\varphi\left(\frac{\sigma_s}{\sigma_f}-1\right)}$

3. Entropy generation analysis

The entropy generation model for nanofluid with a magnetic field can be described as

$$S_{gen} = \frac{k_{nf}}{T_\infty^2}\left(\frac{\partial T}{\partial y}\right)^2 + \frac{\mu_{nf}}{T_\infty}\left(\frac{\partial u}{\partial y}\right)^2 + \frac{\sigma_{nf}B^2}{T_\infty}u^2. \tag{11}$$

The non-dimensional entropy generation S_{GEN} is described as proportion of the volumetric entropy generation (S_{gen}) to the characteristic entropy rate (S_0). Mathematically

$$S_{GEN} = \frac{S_{gen}}{S_0} = \phi_6\left(\frac{\partial T}{\partial y}\right)^2 + \phi_2 Br\Omega^{-1}\left(\frac{\partial u}{\partial y}\right)^2 + \phi_3 Br\Omega^{-1}Mu^2, \tag{12}$$

given that

$$\begin{aligned} S_0 &= \tfrac{k_f(T_w-T_\infty)^2u_0^2}{T_\infty^2\nu_f^2} \quad \text{(Charactersticentropygeneration)}, \\ Br &= \tfrac{\mu_f u_0^2}{k_f(T_w-T_\infty)} \quad \text{(Brinkmannumber)}, \\ \Omega &= \tfrac{T_w-T_\infty}{T_\infty} \quad \text{(Temperaturedifference)}. \end{aligned} \tag{13}$$

Let N_1 and N_2 represent the irreversibility due to heat transport and fluid friction, respectively, then Eq. 12 takes the form

$$S_{GEN} = N_1 + N_2, \tag{14}$$

provided that

$$N_1 = \phi_6\left(\frac{\partial T}{\partial y}\right)^2,\ N_2 = \phi_2 Br\Omega^{-1}\left(\frac{\partial U}{\partial y}\right)^2 + \phi_3 Br\Omega^{-1}Mu^2. \tag{15}$$

The Bejan number (Be) is valuable for evaluating irreversibility distribution. It is a ratio of entropy generation due to heat transfer to overall entropy generation

$$Be = \frac{N_1}{N_1 + N_2}. \tag{16}$$

The Bejan number range is [0,1], $Be = 0$ indicates that N_1 is defeated by N_2 and $Be = 1$ shows that N_1 is dominated by N_2. If the entropy generated by fluid friction and heat transfer contribute equally, the Be value is 0.5.

Table 2 Thermo-physical properties of water and Fe_3O_4 nanoparticle.

Materials	ρ kgm^{-3}	σ Sm^{-1}	β K^{-1}	C_p J(kgK)$^{-1}$	k W(mK)$^{-1}$
Pure water	997.1	0.05	21×10^{-5}	4179	0.613
Fe_3O_4	5200	25000	1.3×10^{-5}	670	6

Table 3 Comparison of values of $\frac{\partial T}{\partial y}|_{y=0}$ for various values of Pr when $\varphi = M = Q = n = 0$ and $Ri = Re = 1$.

Pr	[34]	[35]	[36]	[37]	Present
0.1	0.1637	0.164	0.1629	0.1630	0.1644
1	0.4009	0.401	0.4012	0.4015	0.4093
10	0.8266	0.827	0.8262	0.8274	0.8445

4. Numerical analysis

The numerical solutions have obtained using the finite difference method. Specifically, an implicit, unconditionally stable, Crank–Nicolson method has been utilized to find accurate and convergent solutions [31–33]. If $u_{i,j}^n, v_{i,j}^n$ and $T_{i,j}^n$ represent the approximation of $u(x,y,t), v(x,y,t)$, and $T(x,y,t)$ at time n for any point (x_i, y_j), then the discrete form of Eqs. 6, 7 and 8, are given as

$$v_{i,j}^{n+1} = v_{i,j-1}^{n+1} - v_{i,j}^n + v_{i,j-1}^n - a_1\left(u_{i,j-1}^{n+1} - u_{i-1,j-1}^{n+1} + u_{i,j}^{n+1} - u_{i-1,j}^{n+1} + u_{i,j-1}^n - u_{i-1,j-1}^n + u_{i,j}^n - u_{i-1,j}^n\right), \tag{17}$$

$$-a_2 u_{i-1,j}^{n+1} - b_1 u_{i,j-1}^{n+1} + (1+d_1)u_{i,j}^{n+1} - c_1 u_{i,j+1}^{n+1} = a_2 u_{i-1,j}^{n+1} + b_1 u_{i,j-1}^n (1-d_1)u_{i,j}^n + c_1 u_{i,j+1}^n + f, \tag{18}$$

$$-a_2 T_{i-1,j}^{n+1} - b_2 T_{i,j-1}^{n+1} + (1+d_2)T_{i,j}^{n+1} - c_2 T_{i,j+1}^{n+1} = a_2 T_{i-1,j}^n + b_2 T_{i,j-1}^n + (1-d_2)T_{i,j}^n + c_2 T_{i,j+1}^n, \tag{19}$$

given that

$$\begin{aligned} a_1 &= \tfrac{\Delta y}{2\Delta x},\ a_2 = \tfrac{\Delta t}{2\Delta x}u_{i,j}^n, & f &= \tfrac{\phi_4 Ri Re^{-1}\Delta t}{2\phi_1}\left(T_{i,j}^{n+1} + T_{i,j}^n\right), \\ b_1 &= \tfrac{\phi_2 \Delta t}{2\phi_1 \Delta y^2} + \tfrac{\Delta t}{4\Delta y}v_{i,j}^n, & b_2 &= \tfrac{\phi_6 \Delta t}{2\phi_5 Pr \Delta y^2} + \tfrac{\Delta t}{4\Delta y}v_{i,j}^n, \\ c_1 &= \tfrac{\phi_2 \Delta t}{2\phi_1 \Delta y^2} - \tfrac{\Delta t}{4\Delta y}v_{i,j}^n, & c_2 &= \tfrac{\phi_6 \Delta t}{2\phi_5 Pr \Delta y^2} + \tfrac{\Delta t}{4\Delta y}v_{i,j}^n, \\ d_1 &= \tfrac{\Delta t}{2\Delta x}u_{i,j}^n + \tfrac{\phi_2 \Delta t}{\phi_1 \Delta y^2} + \tfrac{\phi_3 M \Delta t}{2\phi_1}, & d_2 &= \tfrac{\Delta t}{2\Delta x}u_{i,j}^n + \tfrac{\phi_6 \Delta t}{\phi_5 Pr \Delta y^2} + \tfrac{Q\Delta t}{2\phi_5}. \end{aligned} \tag{20}$$

At each i, the discrete Eqs.18 and 19 give us tri-diagonal systems, further solved by Thomas algorithm in MATLAB Software. The integration area has been taken as a rectangular with limits $x_{max} = 1$ and $y_{max} = 15$ such that it takes a location far away from the thermal and momentum boundary layers, here y_{max} refers to $y = \infty$. The mesh sizes are taken as $\Delta x = \Delta y = 0.05$ and the time level is considered $\Delta t = 0.01$. Numerical iterations have been repeated several times to obtain convergent solutions. For a convergent solution, the tolerance rate has been taken as $1e^{-5}$. Moreover, Table 3 ensures validation of the present numerical solution with the existing study for steady case with zero velocity conditions at the wall.

5. Graphical results and discussion

The effect of cylindrical-shaped Fe_3O_4 nanoparticles on mixed convection heat transfer and entropy generation in an electrically conducting ferrofluid over a vertical surface in the presence of heat generation is studied. The thermal conductivity of cylindrical-shaped nanoparticles is estimated using Hamilton and Crosser [38].

The effects of involved parameters on fluid flow and heat transfer features of ferrofluid are presented graphically. The numerical values assigned to the fixed parameters are: $Pr = 6.2, \varphi = 0.01, M = 3, Ri = 1, Re = 0.1, Q = 1,$ and $n = 0.5$. The range of parameters are: $0 \leqslant \varphi \leqslant 0.04$, $0 \leqslant M \leqslant 7, 0 \leqslant Q \leqslant 1.5$ and $0 \leqslant n \leqslant 1$. The results are logical and closer to physical expectations.

The variation in the temperature and velocity profiles of ferrofluid due to the volumetric concentration of cylindrical-shaped Fe_3O_4 nanoparticles are depicted in Figs. 2 and 3, respectively. A significant increment in temperature is observed on suspending tiny nanoparticles in the base fluid, see Fig. 2. This relation is close to physical expectation since the suspension of nanoparticles increases the temperature due to increased thermal conductivity. On the other hand, the velocity of ferrofluid showed a dual nature under the variation of volumetric concentration of Fe_3O_4 nanoparticles, displayed in Fig. 3. The flow profile decrease with an increment in nanoparticle volume fraction when $y \lessapprox 1$ and increases by adding more particles when $y \gtrapprox 1$. The effects of the magnetic field on the temperature and velocity profiles of ferrofluid are plotted in Figs. 4 and 5, respectively. The result ensures a significant increment in the temperature for higher values of M. An opposite behavior is noticed on the velocity profile. This behavior was evident because the magnetic field generates resistive Lorentz force and an increment in the value of M also intensifies the resistive forces. Due to this fact, the velocity profile

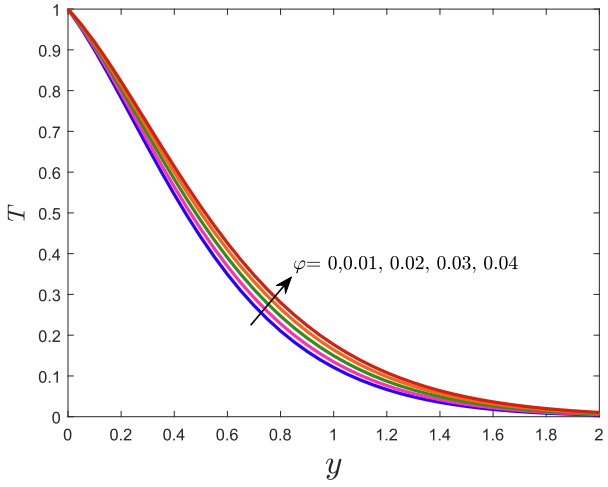

Fig. 2 Influence of φ on temperature profile.

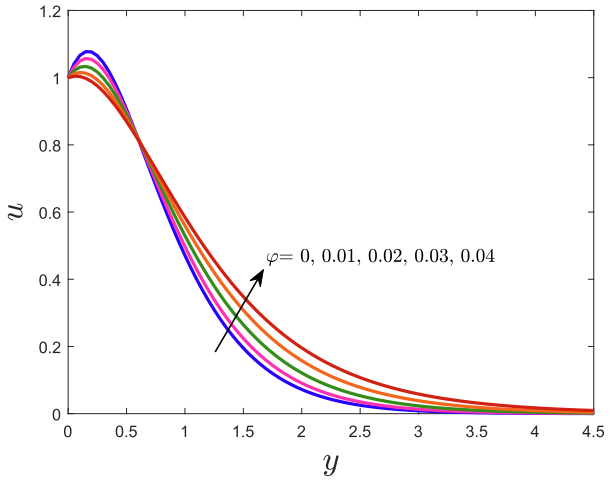

Fig. 3 Influence of φ on velocity profile.

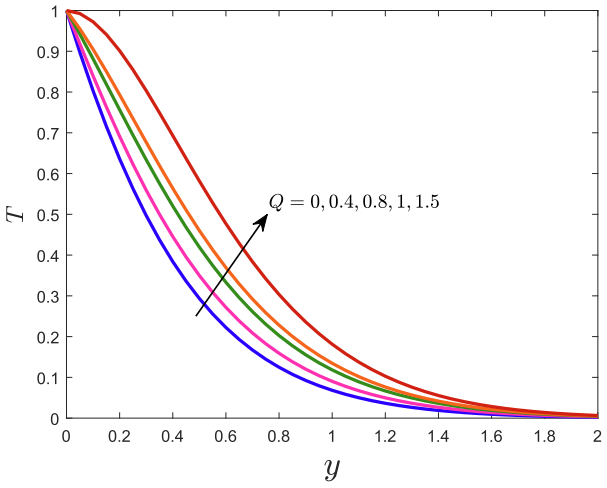

Fig. 6 Influence of Q on temperature profile.

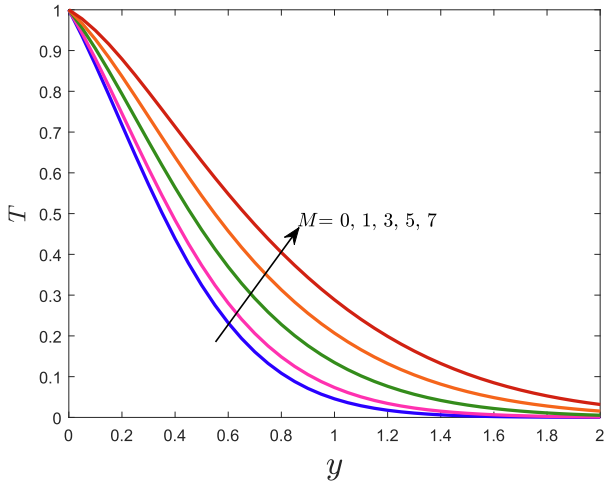

Fig. 4 Influence of M on temperature profile.

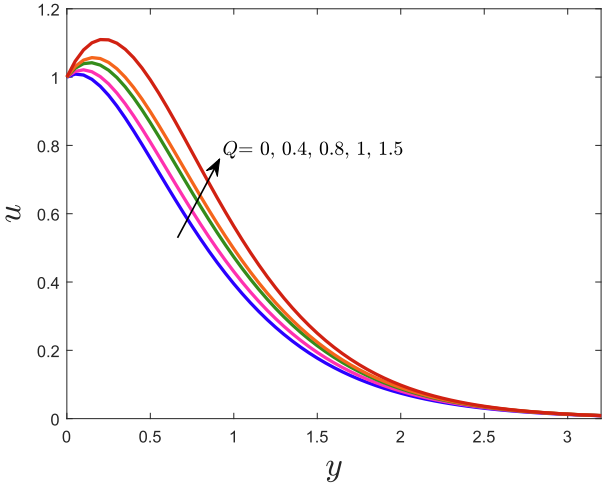

Fig. 7 Influence of Q on velocity profile.

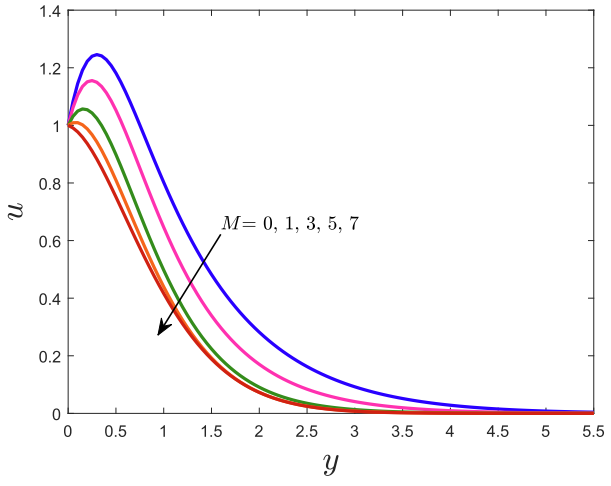

Fig. 5 Influence of M on velocity profile.

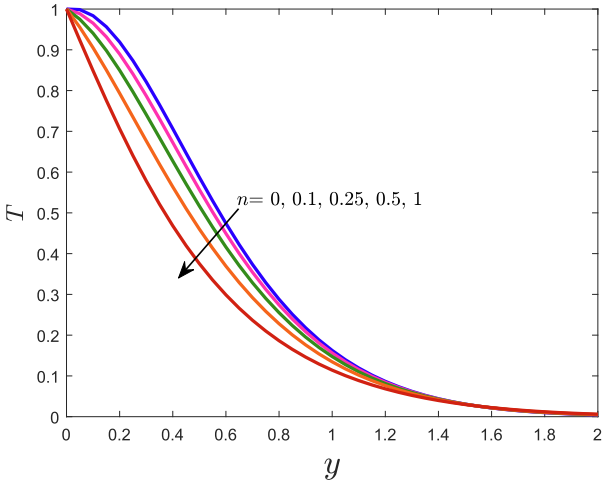

Fig. 8 Influence of n on temperature profile.

dropped off against the magnetic field. Figs. 6 and 7 reveal the nature of temperature and velocity of ferrofluid under the effects of heat generation parameter, respectively. Fig. 6 shows that maximum temperature is attained by increasing the value of the heat generation parameter Q. Physically, when heat is generated, the temperature rise is evident. In Fig. 7, the trend of velocity curves confirmed an increment in the buoyancy force occurs due to heat generation; as a result, the velocity profile escalates significantly. The effects of the power index on the thermal and momentum boundary layer are plotted in Figs. 8 and 9, respectively. It is evident from the illustrated results that an increment in the power index parameter decreases the thermal and momentum boundary layer.

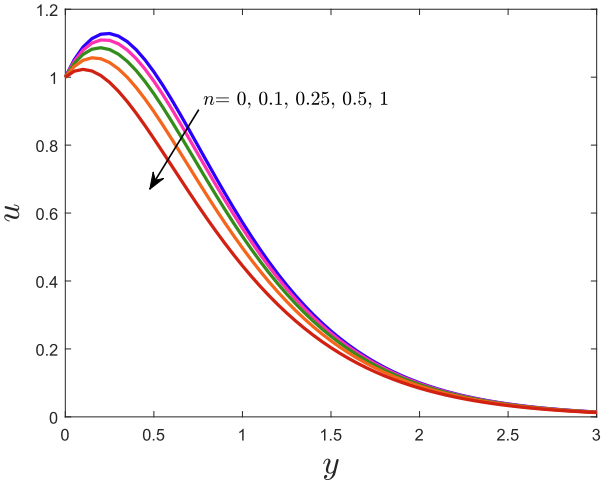

Fig. 9 Influence of n on velocity profile.

Figs. 10–17 are illustrated to analyze the variations in entropy generation and Bejan lines for different parameters. Fig. 10 exhibits the change in the entropy generation rate caused by the addition of nanoparticles to the base fluid. The entropy generation S_{GEN} is observed to grow with φ. The changes in Bejan number Be for different volume fractions of nanoparticles are shown in Fig. 11. For all cases analyzed, Be reduces as φ increases, indicating that adding nanoparticles to the base fluid increases the friction irreversibility rate. It is noted that a rise in Lorentz force tends to encourage the enhancement rate of entropy generation, as shown in Fig. 12. Furthermore, Be falls as the magnetic number rises, see Fig. 13. It reveals that lowering the magnetic number reduces the rate of irreversible heat transfer relative to friction. Fig. 14 shows that the entropy rate increases when the Brinkman number Br increases. Generally, thermal conductivity reduces when the Brinkman number grows, which increases entropy generation. On the other hand, the Bejan number decreases when Br increases, displayed in Fig. 15. The influence of temperature difference parameter Ω on entropy generation and Bejan number are depicted in Figs. 16 and 17, respectively. The entropy generation rate reduced when Ω increased. At the same time, the Bejan number increased with the rise in Ω.

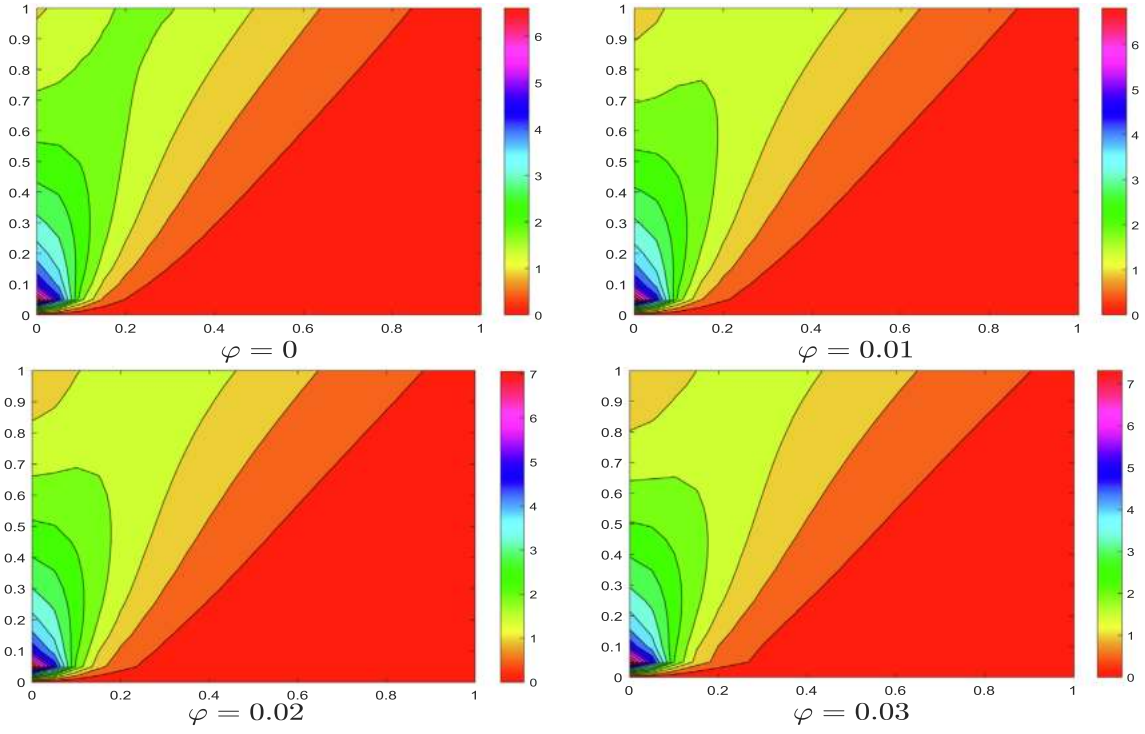

Fig. 10 Entropy generation for various values of φ.

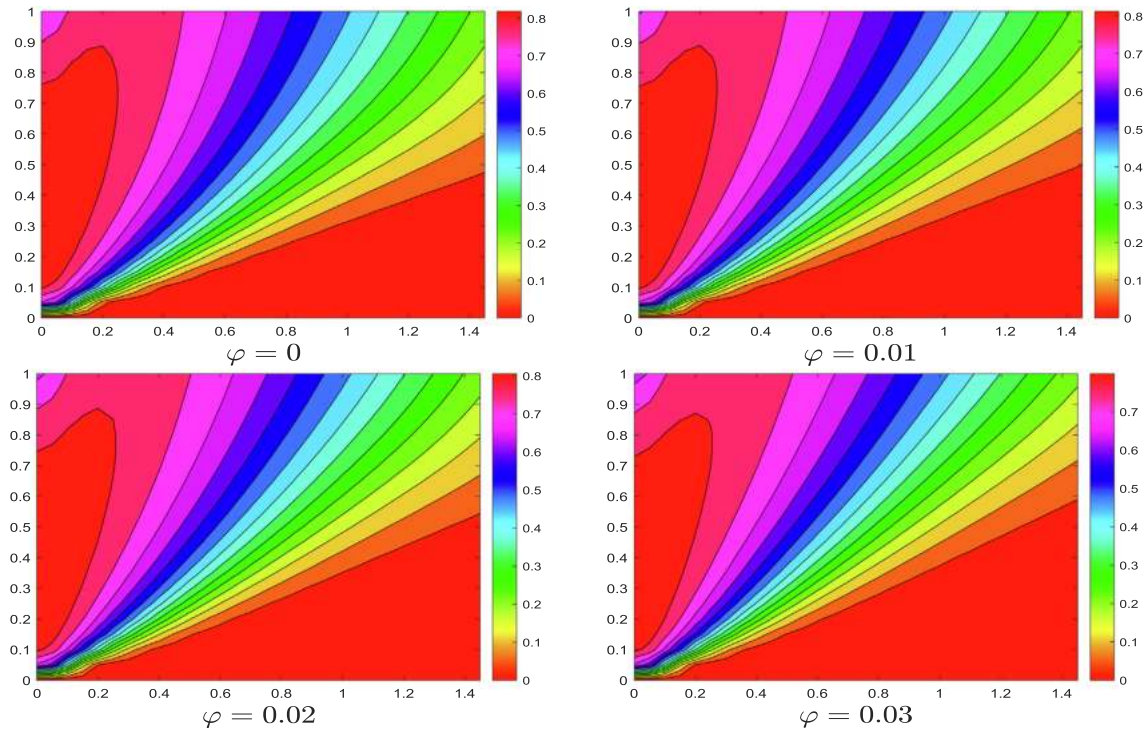

Fig. 11 Bejan lines for various values of φ.

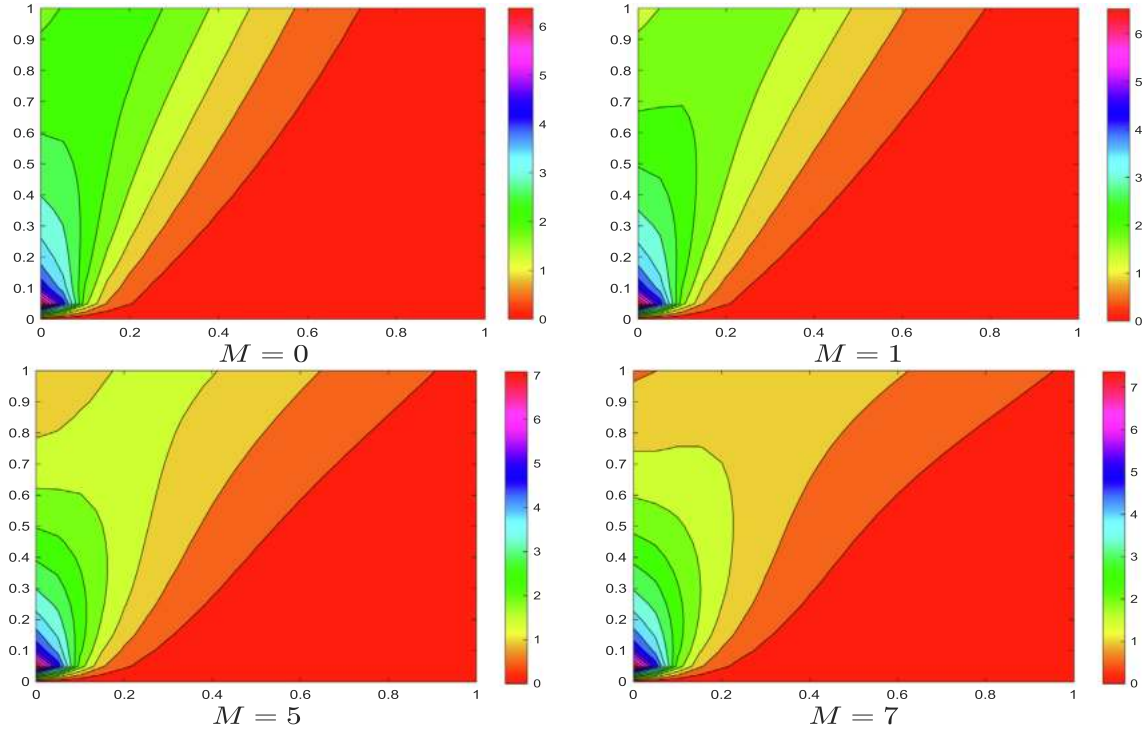

Fig. 12 Entropy generation for various values of M.

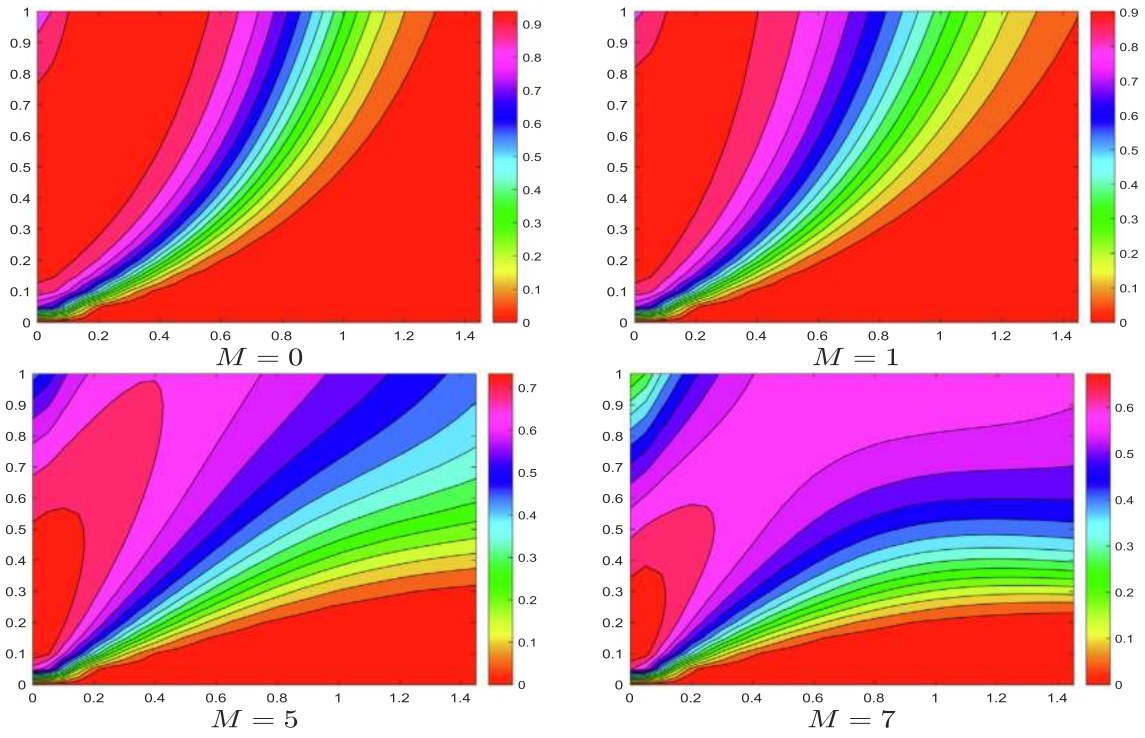

Fig. 13 Bejan lines for various values of M.

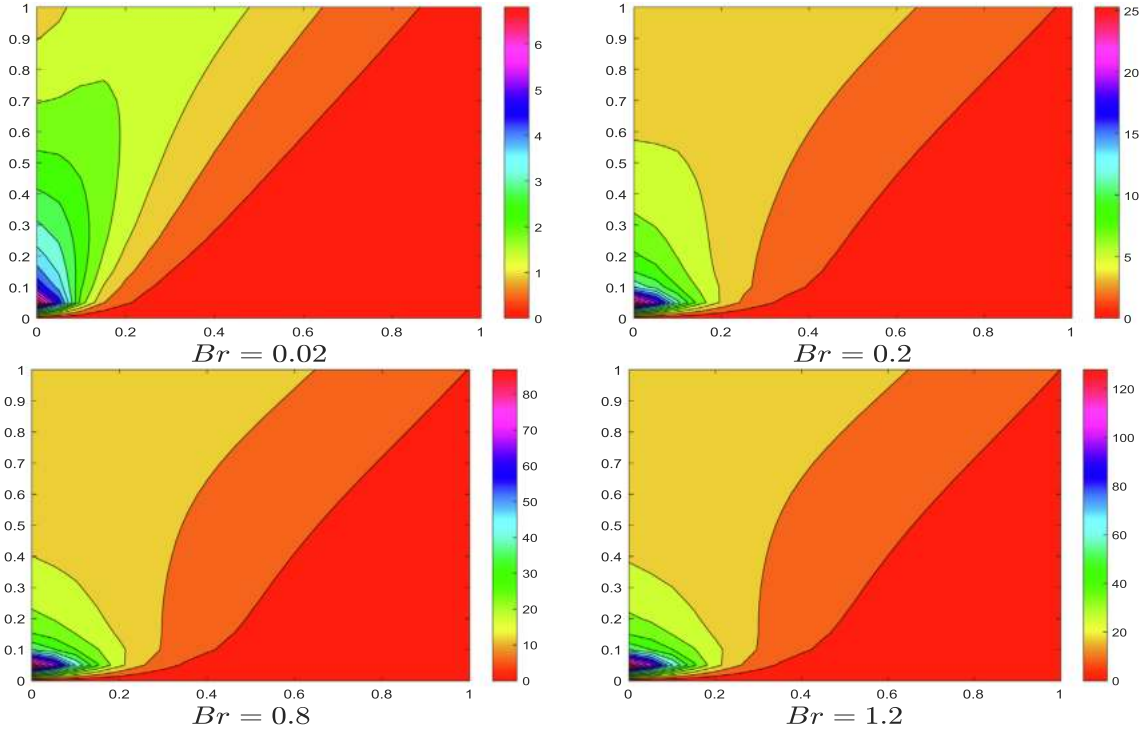

Fig. 14 Entropy generation for various values of Br.

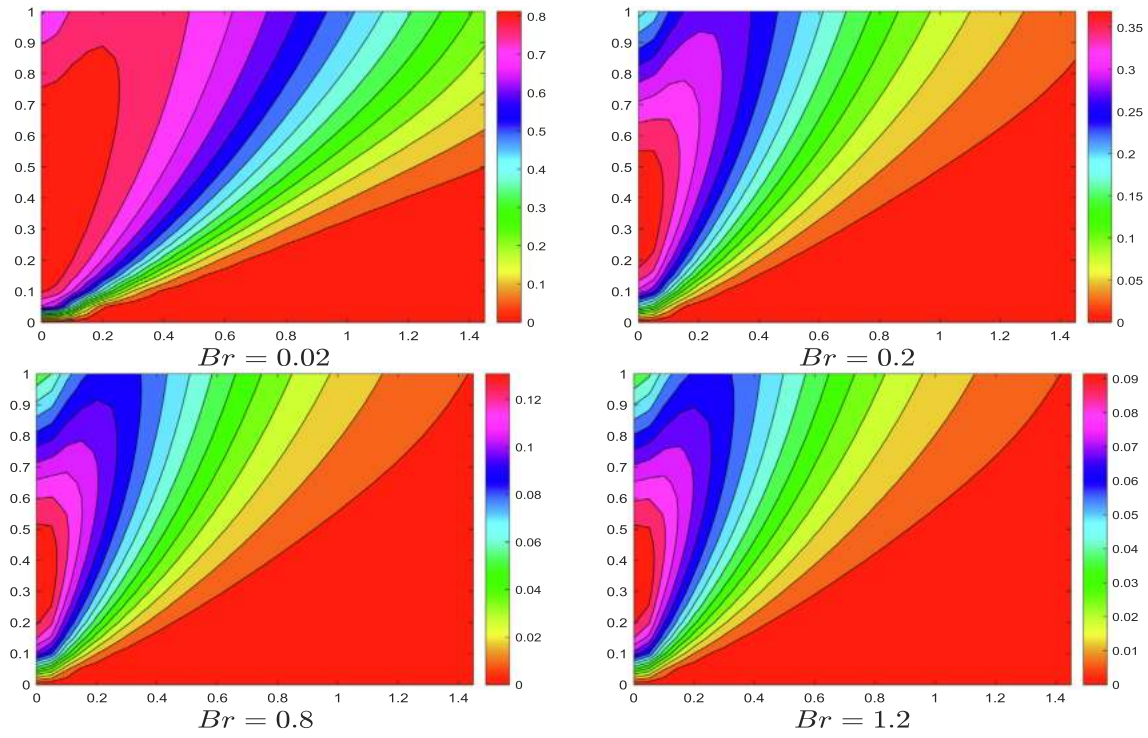

Fig. 15 Bejan lines for various values of *Br*.

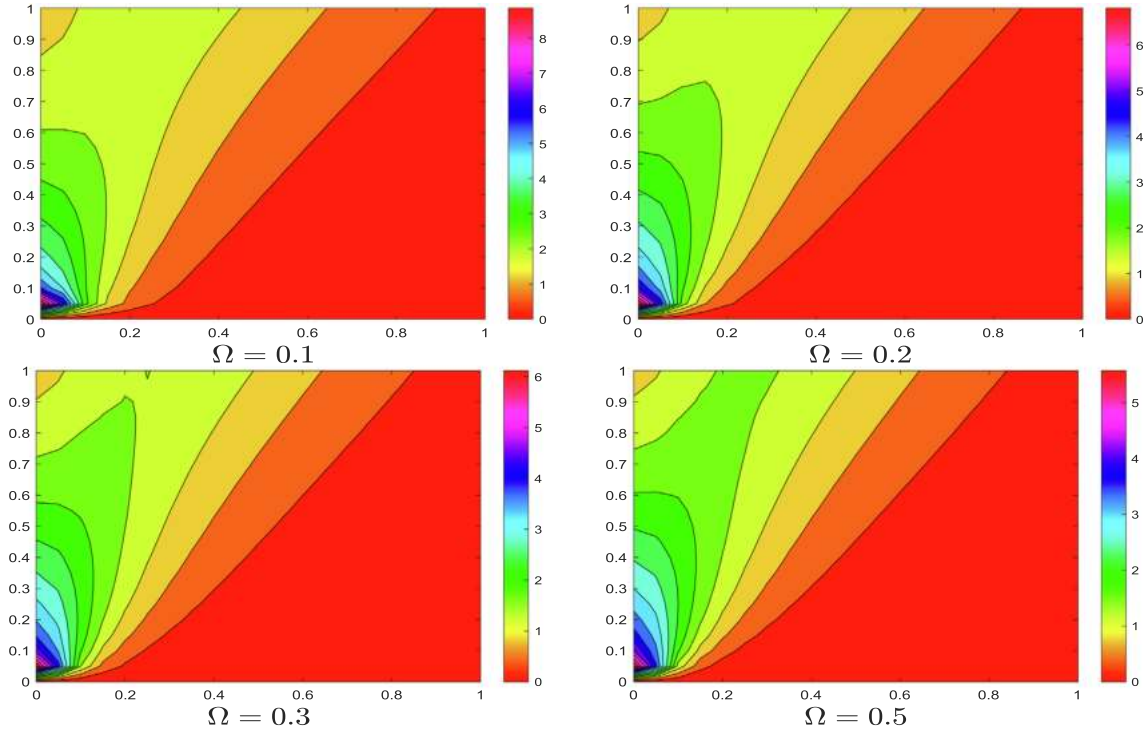

Fig. 16 Entropy generation for various values of Ω.

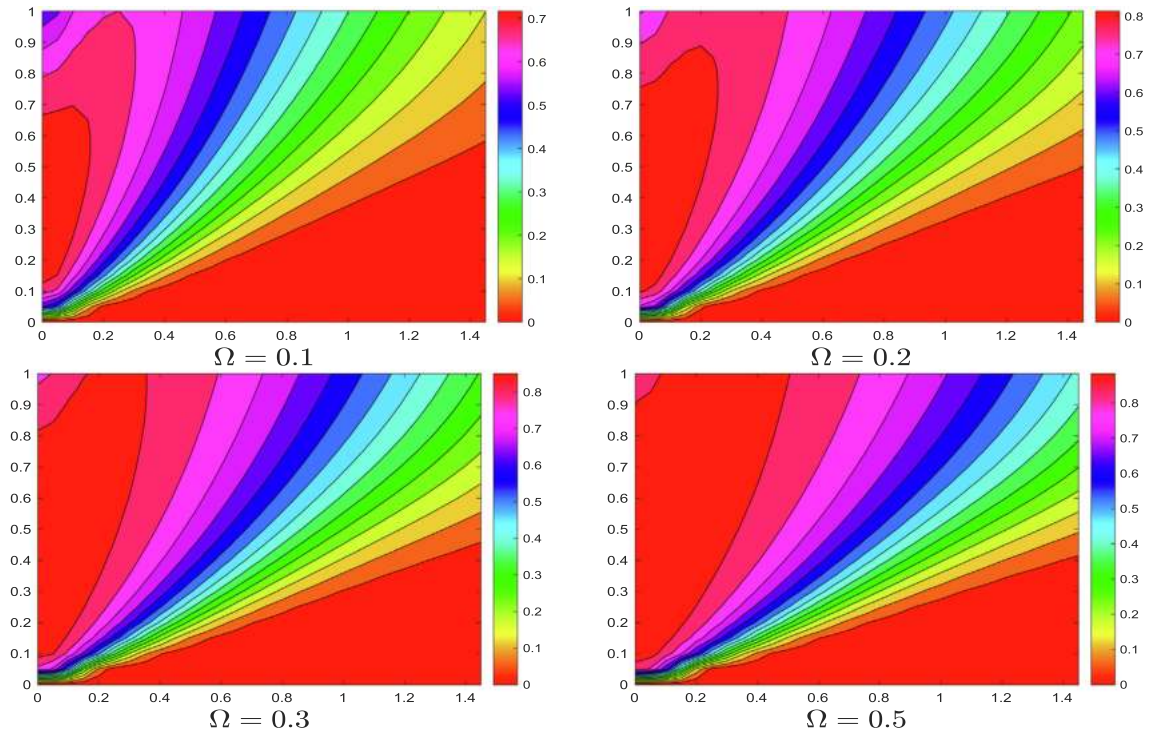

Fig. 17 Bejan lines for various values of Ω.

6. Conclusions

Entropy generation in a two-dimensional ferrofluid flow over a flat surface with variable wall temperature is analyzed. Additionally, the impacts of the magnetic field together with heat generation/absorption are also investigated. An implicit finite difference is utilized to obtain the numerical solutions. The results showed that:

- The temperature profile is lifted up by adding nano-sized Fe_3O_4 particles. Physically the suspension of nanoparticles improves the thermal conductivity of the regular base fluid (water), consequently, the temperature.
- The Fe_3O_4 nanoparticles diminished the velocity profile when $y \lessapprox 1$.
- The temperature distribution and the velocity profile attained maximum values when heat is generated.
- The entropy generation increases with the Brinkman number; however, the entropy generation decreases as the temperature difference grows.
- The friction irreversibility rate increased when the nanoparticle volume fraction and magnetic parameter increased.

Declaration of Competing Interest

The authors declare that they have no known competing financial interests or personal relationships that could have appeared to influence the work reported in this paper.

Acknowledgment

The authors would like to acknowledge the Ministry of Higher Education Malaysia and Research Management Centre-UTM, Universiti Teknologi Malaysia (UTM) for financial support through vote numbers 08G33.

References

[1] S.U. Choi, J.A. Eastman, Enhancing thermal conductivity of fluids with nanoparticles, Technical Report, Argonne National Lab, IL (United States), 1995.

[2] W. Jamshed, M.R. Eid, A. Aissa, A. Mourad, K.S. Nisar, F. Shahzad, C.A. Saleel, V. Vijayakumar, Partial velocity slip effect on working magneto non-newtonian nanofluids flow in solar collectors subject to change viscosity and thermal conductivity with temperature, Plos one 16 (2021) e0259881, https://doi.org/10.1371/journal.pone.0259881.

[3] H. Hanif, A finite difference method to analyze heat and mass transfer in kerosene based γ-oxide nanofluid for cooling applications, Phys. Scr. 96 (2021) 095215, https://doi.org/10.1088/1402-4896/ac098a.

[4] A.S. Dogonchi, S. Mishra, N. Karimi, A.J. Chamkha, H. Alhumade, Interaction of fusion temperature on the magnetic free convection of nano-encapsulated phase change materials within two rectangular fins-equipped porous enclosure, J. Taiwan Inst. Chem. Eng. 124 (2021) 327–340, https://doi.org/10.1016/j.jtice.2021.03.010.

[5] T. Zubair, M. Usman, M. Hamid, M. Sohail, U. Nazir, K.S. Nisar, V. Vijayakumar, Computational analysis of radiative williamson hybrid nanofluid comprising variable thermal conductivity, Jpn. J. Appl. Phys. 60 (2021) 087004, https://doi.org/10.35848/1347-4065/ac1388.

[6] P. Pattnaik, M. Bhatti, S. Mishra, M.A. Abbas, O.A. Bég, Mixed convective-radiative dissipative magnetized micropolar nanofluid flow over a stretching surface in porous media with double stratification and chemical reaction effects: Adm-Padé computation, J. Math. 2022 (2022), https://doi.org/10.1155/2022/9888379.

[7] H. Hanif, S. Shafie, Interaction of multi-walled carbon nanotubes in mineral oil based Maxwell nanofluid, Scientific

Reports 12 (2022) 1–16, https://doi.org/10.1038/s41598-022-07958-y.
[8] P. Pattnaik, J. Pattnaik, S. Mishra, K.S. Nisar, Variation of the shape of Fe_3O_4-nanoparticles on the heat transfer phenomenon with the inclusion of thermal radiation, J. Therm. Anal. Calorim. 147 (2022) 2537–2548, https://doi.org/10.1007/s10973-021-10605-9.
[9] H. Hanif, I. Khan, S. Shafie, A novel study on hybrid model of radiative Cu–Fe_3O_4/water nanofluid over a cone with PHF/PWT, The European Physical Journal Special Topics 230 (2021) 1257–1271, https://doi.org/10.1140/epjs/s11734-021-00042-y.
[10] F. Shahzad, W. Jamshed, T. Sajid, K.S. Nisar, M.R. Eid, Heat transfer analysis of mhd rotating flow of Fe_3O_4 nanoparticles through a stretchable surface, Commun. Theor. Phys. 73 (2021) 075004, https://doi.org/10.1088/1572-9494/abf8a1.
[11] M. Li, L. Zhu, Interfacial instability of ferrofluid flow under the influence of a vacuum magnetic field, Applied Mathematics and Mechanics 42 (2021) 1171–1182, https://doi.org/10.1007/s10483-021-2758-7.
[12] N. Acharya, Spectral simulation to investigate the effects of nanoparticle diameter and nanolayer on the ferrofluid flow over a slippery rotating disk in the presence of low oscillating magnetic field, Heat Transfer 50 (2021) 5951–5981, https://doi.org/10.1002/htj.22157.
[13] H. Hanif, I. Khan, S. Shafie, A novel study on time-dependent viscosity model of magneto-hybrid nanofluid flow over a permeable cone: Applications in material engineering, The European Physical Journal Plus 135 (2020) 730, https://doi.org/10.1140/epjp/s13360-020-00724-x.
[14] H. Hanif, S. Shafie, Impact of Al_2O_3 in electrically conducting mineral oil-based Maxwell nanofluid: Application to the petroleum industry, Fractal and Fractional 6 (2022) 180, https://doi.org/10.3390/fractalfract6040180.
[15] H. Hanif, S. Shafie, Application of Cattaneo heat flux to maxwell hybrid nanofluid model: a numerical approach, The European Physical Journal Plus 137 (2022) 989, https://doi.org/10.1140/epjp/s13360-022-03209-1.
[16] P.K. Pattnaik, M.A. Abbas, S. Mishra, S.U. Khan, M.M. Bhatti, Free convective flow of hamilton-crosser model gold-water nanofluid through a channel with permeable moving walls, Combinatorial Chemistry & High Throughput Screening 25 (2022) 1103–1114, https://doi.org/10.2174/1386207324666210813112323.
[17] M. Saqib, H. Hanif, T. Abdeljawad, I. Khan, S. Shafie, K.S. Nisar, Heat transfer in MHD flow of Maxwell fluid via fractional Cattaneo-Friedrich model: A finite difference approach, Comput. Mater. Contin 65 (2020) 1959–1973, https://doi.org/10.32604/cmc.2020.011339.
[18] H. Hanif, I. Khan, S. Shafie, W.A. Khan, Heat transfer in cadmium telluride-water nanofluid over a vertical cone under the effects of magnetic field inside porous medium, Processes 8 (2019) 7, https://doi.org/10.3390/pr8010007.
[19] Y.-X. Li, S. Mishra, P. Pattnaik, S. Baag, Y.-M. Li, M.I. Khan, N.B. Khan, M.K. Alaoui, S.U. Khan, Numerical treatment of time dependent magnetohydrodynamic nanofluid flow of mass and heat transport subject to chemical reaction and heat source, Alexandria Engineering Journal 61 (2022) 2484–2491, https://doi.org/10.1016/j.aej.2021.07.030.
[20] H. Hanif, I. Khan, S. Shafie, MHD natural convection in cadmium telluride nanofluid over a vertical cone embedded in a porous medium, Phys. Scr. 94 (2019) 125208, https://doi.org/10.1088/1402-4896/ab36e1.
[21] O. Mahian, A. Kianifar, C. Kleinstreuer, A.-N. Moh'd A, I. Pop, A.Z. Sahin, S. Wongwises, A review of entropy generation in nanofluid flow, Int. J. Heat Mass Transf. 65 (2013) 514–532, https://doi.org/10.1016/j.ijheatmasstransfer.2013.06.010.
[22] R. Khosravi, S. Rabiei, M. Khaki, M.R. Safaei, M. Goodarzi, Entropy generation of graphene–platinum hybrid nanofluid flow through a wavy cylindrical microchannel solar receiver by using neural networks, J. Therm. Anal. Calorim. 145 (2021) 1949–1967, https://doi.org/10.1007/s10973-021-10828-w.
[23] S. Marzougui, F. Mebarek-Oudina, A. Assia, M. Magherbi, Z. Shah, K. Ramesh, Entropy generation on magneto-convective flow of copper–water nanofluid in a cavity with chamfers, J. Therm. Anal. Calorim. 143 (2021) 2203–2214, https://doi.org/10.1007/s10973-020-09662-3.
[24] W. Jamshed, Numerical investigation of MHD impact on Maxwell nanofluid, Int. Commun. Heat Mass Transfer 120 (2021) 104973, https://doi.org/10.1016/j.icheatmasstransfer.2020.104973.
[25] T. Tayebi, A.S. Dogonchi, N. Karimi, H. Ge-JiLe, A.J. Chamkha, Y. Elmasry, Thermo-economic and entropy generation analyses of magnetic natural convective flow in a nanofluid-filled annular enclosure fitted with fins, Sustainable Energy Technologies and Assessments 46 (2021) 101274, https://doi.org/10.1016/j.seta.2021.101274.
[26] M. Nakhchi, M. Rahmati, Entropy generation of turbulent Cu–water nanofluid flows inside thermal systems equipped with transverse-cut twisted turbulators, J. Therm. Anal. Calorim. 143 (2021) 2475–2484, https://doi.org/10.1007/s10973-020-09960-w.
[27] W. Jamshed, S. Mishra, P. Pattnaik, K.S. Nisar, S.S.U. Devi, M. Prakash, F. Shahzad, M. Hussain, V. Vijayakumar, Features of entropy optimization on viscous second grade nanofluid streamed with thermal radiation: A tiwari and das model, Case Studies in Thermal Engineering 27 (2021) 101291, https://doi.org/10.1016/j.csite.2021.101291.
[28] H. Hanif, I. Khan, S. Shafie, Heat transfer exaggeration and entropy analysis in magneto-hybrid nanofluid flow over a vertical cone: a numerical study, J. Therm. Anal. Calorim. 141 (2020) 2001–2017, https://doi.org/10.1007/s10973-020-09256-z.
[29] A. Cuadras, P. Miró, V.J. Ovejas, F. Estrany, Entropy generation model to estimate battery ageing, Journal of Energy Storage 32 (2020) 101740, https://doi.org/10.1016/j.est.2020.101740.
[30] S.M. Hussain, W. Jamshed, A comparative entropy based analysis of tangent hyperbolic hybrid nanofluid flow: Implementing finite difference method, Int. Commun. Heat Mass Transfer 129 (2021) 105671, https://doi.org/10.1016/j.icheatmasstransfer.2021.105671.
[31] H. Hanif, Cattaneo-Friedrich and Crank-Nicolson analysis of upper-convected Maxwell fluid along a vertical plate, Chaos, Solitons & Fractals 153 (2021) 111463, https://doi.org/10.1016/j.chaos.2021.111463.
[32] J. Crank, P. Nicolson, A practical method for numerical evaluation of solutions of partial differential equations of the heat-conduction type, in: Mathematical proceedings of the Cambridge philosophical society, volume 43, Cambridge University Press, pp. 50–67. doi: 10.1007/BF02127704.
[33] H. Hanif, A computational approach for boundary layer flow and heat transfer of fractional Maxwell fluid, Mathematics and Computers in Simulation 191 (2022) 1–13, https://doi.org/10.1016/j.matcom.2021.07.024.
[34] T. Cebeci, P. Bradshaw, Physical and computational aspects of convective heat transfer, Springer, 1984, https://doi.org/10.1007/978-1-4612-3918-5.
[35] W.M. Kays, M.E. Crawford, B. Weigand, Convective heat and mass transfer, volume 4, McGraw-Hill New York, 1980.

[36] K. Yih, Effect of radiation on natural convection about a truncated cone, Int. J. Heat Mass Transf. 42 (1999) 4299–4305, https://doi.org/10.1016/S0017-9310(99)00092-7.

[37] A.J. Chamkha, A. Rashad, H.F. Al-Mudhaf, Heat and mass transfer from truncated cones with variable wall temperature and concentration in the presence of chemical reaction effects, Int. J. Numer. Methods Heat Fluid Flow (2012), https://doi.org/10.1108/09615531211208060.

[38] R.L. Hamilton, O. Crosser, Thermal conductivity of heterogeneous two-component systems, Industr. Eng. Chem. Fundam. 1 (1962) 187–191.